Pore Pressure in the Lokvarka Dam

Pressions Interstitielles dans le Barrage de Lokvarka

by E. NONVEILLER, C.E., Geoistraživanja, Kupska 2, Zagreb, Yugoslavia

Summary

The 48 m high, 280 m long Lokvarka dam consists of a sloping clay core of silty clay supported on the upstream side by a rock-fill shell, and on the downstream side by a semi-pervious fill. The foundation consists partly of impervious carboniferous schist, partly of pervious dolomite rock. The construction began in 1952 and was completed in 1955.

Geotechnical characteristics of the clay and results of triaxial tests with pore pressure measurements are given.

Pore pressure cells were installed in the core. The readings show low construction pore pressure. Records at different water elevations show that the pressures and the pattern of the flow net change rapidly. Overall pore pressure coefficient, $\bar{B}$, calculated from pore pressure records in this dam, are very different from the laboratory results obtained.

Records on this and other dams show that the actual flow nets agree fairly well with the theoretical patterns for rapid draw-down.

It seems that the calculation of active forces in stability analyses can be based on pore pressures from flow nets before and after rapid draw-down.

Sommaire

Le barrage de Lokvarka, de 48 m de hauteur et 280 m de longueur, comporte un noyau étanche en argile sableuse soutenu par un enrochement en amont et par un remblai sémiperméable en aval. La fondation est composée de schiste carbonifère imperméable et partiellement de dolomite perméable. La construction commença en 1952 et fut terminée en 1955.

On donne les caractéristiques géotechniques de l'argile et les résultats des mesures de la pression interstitielle sur des échantillons triaxiaux.

Des témoins sonores pour pressions interstitielles sont placés dans le noyau. Les observations pendant la construction montrent des pressions interstitielles basses, tandis que celles faites à des niveaux différents dans la retenue indiquent que les pressions et les réseaux potentiels changent rapidement.

Le coefficient de la pression interstitielle $\bar{B}$ calculé d'après les observations dans ce barrage est bien différent des valeurs obtenues au laboratoire. Les observations indiquent que les réseaux potentiels réels pour vidange rapide correspondent bien au schéma théorique.

Il semble que la détermination des forces actives pour le calcul de la stabilité des barrages après vidange rapide peut se faire d'après les valeurs des pressions interstitielles correspondant aux schémas théoriques des réseaux potentiels.

Description of the Dam

The main storage basin of the hydroelectric power plant 'Nikola Tesla' is formed by the earth dam Lokvarka (NONVEILLER, 1954). The dam is 48 m high with a crest length of 280 m and a volume of 673,000 m^3. Fig. 1 shows the completed

Fig. 1 Lokvarka dam
Barrage Lokvarka

dam and Fig. 2 its cross-section. In accordance with the available materials a type of dam with a relatively thin impermeable core of silty clay in the upstream portion of the dam was chosen. The upstream retaining portion is of a very coarse dolomite rock. A three-layer filter of crushed rock gravel and sand, 3 m thick, forms the transition to the core. The downstream part of the dam is built of soft, partly decomposed carboniferous schist. A strong rock-fill downstream toe, drainage layers and drains, assure a satisfactory lowering of the upper flow line in the downstream portion of the dam. All the drains end in a well on the downstream side, in which the amount of the percolating water can be measured. The waste material from the quarry and the borrow area has been placed on the downstream face of the dam. Thus the slope was flattened and was later planted with grass and other growth. The average slope upstream is 1:1·85, downstream 1:2·0 and the slope of the core 1:0·8.

The foundation of the dam is on broken, carboniferous schists of low permeability. On the right abutment the foundation rock is a broken, very permeable dolomite, which has been intersected by a deep concrete wall. An impervious grout curtain, 20 m deep, has been injected below the core. The observations carried out so far show that the foundation is completely impervious.

Geotechnical Characteristics of the Materials

The characteristics of the clay for the core are given in Table 1. In connection with the study of the pore pressure in the core, triaxial tests on specimens compacted like the core material have been carried out. The samples were allowed to come to equilibrium with water percolating through them under values of total major and minor principal stress and pore pressure corresponding to a typical element under the steady seepage condition. Then the drainage was closed, the principal stresses were lowered to the values which correspond to the lowered water surface and the pore pressure measured. After that, the vertical load was increased to failure, and the pore pressure measured simultaneously. The results are shown in Fig. 3 as well as in Table 2.

A value of $\bar{B} = 0{\cdot}50$ corresponds to the stresses for the case

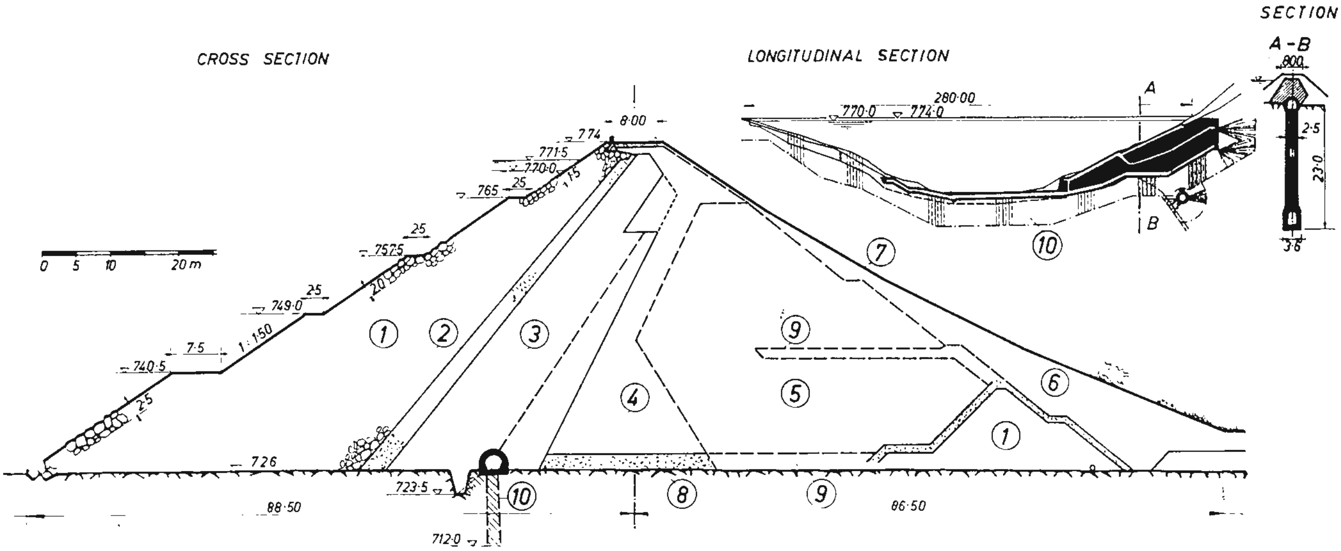

Fig. 2 Cross-section

1 Rock fill 181,000 m³
2 Transition filter 29,000 ,,
3 Clay core 93,000 ,,
4 Décomposed schist
5 Selected schist 323,000 ,,
6 Quarry waste 47,000 ,,
Total 673,000 m³
7 Planted downstream slope
8 Drainage blanket
9 Drainage layers
10 Grouting curtain, 5200 m of bore holes

Section transversale

1 Enrochement 181,000 m³
2 Filtres de transition 29,000 ,,
3 Noyau étanche 93,000 ,,
4 Schiste décomposé
5 Schiste sélectionné 323,000 ,,
6 Tout venant 47,000 ,,
Total 673,000 m³
7 Talus (Parment) aval planté
8 Base filtrante
9 Drainages
10 Injections d'étanchement, au total 5200 m de forages

Table 1

Classification AC	*ML*	*MI*
Liquid limit	30%	40·5%
Plasticity index	5%	10·5%
Grain size 0·1 mm	75%	88%
0·01 mm	18%	32%
0·002 mm	6%	12%
Optimum density t/m³	1·62	1·72
Optimum water content %	22·5	18·5
Coefficient of compressibility m_v cm²/kg⁻¹		
for expansion 8–4 kg/cm²	+ 0·00032	+ 0·00031
8–2 ,,	+ 0·00032	+ 0·00061
for re-compression:		
0·1–0·5 kg/cm²	− 0·0034	− 0·031
0·5–1·0 ,,	− 0·0012	− 0·016
1·0–2·0 ,,	− 0·0024	− 0·010
2·0–4·0 ,,	− 0·0033	− 0·007
4·0–8·0 ,,	—	− 0·010
Permeability k cm/sec	6×10^{-7}	3×10^{-8}
Angle of friction, virgin compression drained test	32°	18°
Angle of cohesion (Krey–Tiedeman)	4·5°	6°

Table 2

Pore pressure coefficient $\bar{B} = \frac{\Delta u}{\Delta \sigma_1}$ (Skempton, 1954)

Coefficients des pressions interstitielles $\bar{B} = \frac{\Delta u}{\Delta \sigma_1}$ (Skempton, 1954)

Sample	4503–1		4503–2		4503–3		
Condition:	*a*	*b*	*a*	*b*	*a*	*b*	*c*
σ_3 lb./sq. in.	50	18·0	48	18·0	30·8	9·0	12·0
σ_1 lb./sq. in.	62	33·2	60	33·2	50·0	32·0	32·0
u lb./sq. in.	30	16·0	30	15·5	16·5	6·0	10·0
Δu lb./sq. in.	—	− 14·0	—	− 14·5	—	− 10·5	− 6·5
$\Delta \sigma_1$ lb./sq. in.	—	− 28·8	—	− 26·8	—	− 18·0	− 18·0
$\bar{B}$	—	0·49	—	0·54	—	0·58	—
B	—	—	—	—	—	—	0·36

Explanation:

(a) Sample allowed to come to equilibrium with water percolating at pressures:

upper end $p_1 = 30$— / lower end $p_2 = 27$ lb./sq. in. } samples 4503–1 and 2
$p_1 = 16{\cdot}5$ / $p_2 = 14$ lb./sq. in. } sample 4503–3

(b) Lowering of stresses σ_1 and σ_3 with drainages closed;

(c) Lowering of stresses to $\Delta\sigma_1 = \Delta\sigma_3$, for determination of coefficient B.

of the lowered water level, but the coefficient changes if the sample is loaded vertically. In Fig. 3c the change of $\bar{B}$ when loading a laterally unloaded sample is given in relation to $(\sigma_1 + \Delta\sigma_1):\sigma_1$ where σ_1 is the axial stress and $\Delta\sigma_1$ the consecutive changes of the axial stress. For all the three samples a practically identical hyperbolic curve has been obtained.

According to this the coefficient $\bar{B}$ seems to be a variable depending on the kind of material and on stress changes. The results obtained will be compared later with the coefficient $\bar{B}$ resulting from pressure measurements in the dam core during a rapid draw-down.

Description of the Measuring Installation

In the dam and on its slopes control installations have been placed for the measurement of deformation of the dam and its

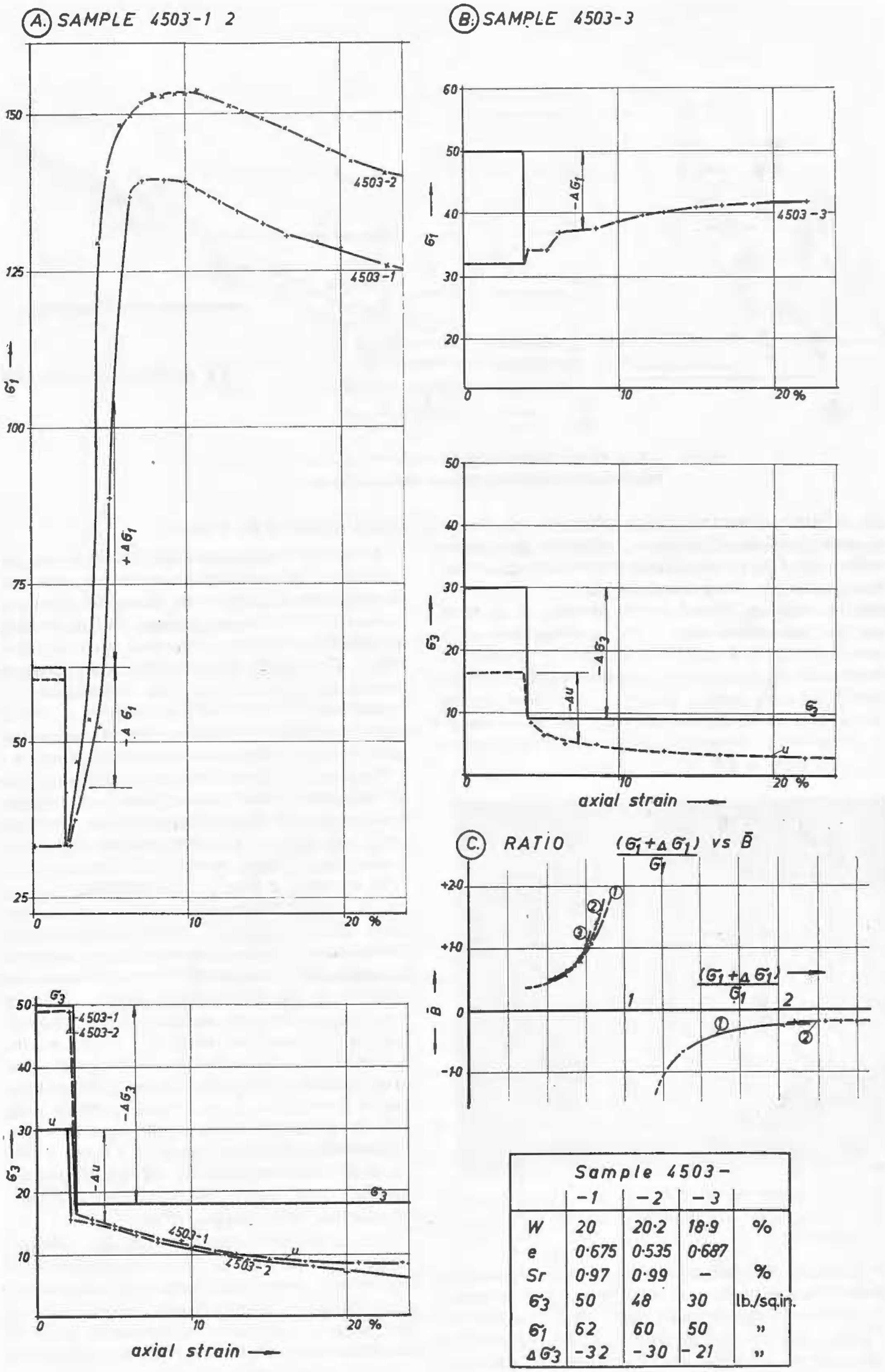

	Sample 4503-			
	-1	-2	-3	
W	20	20·2	18·9	%
e	0·675	0·535	0·687	
Sr	0·97	0·99	–	%
σ_3	50	48	30	lb./sq.in.
σ_1	62	60	50	”
$\Delta\sigma_3$	-32	-30	- 21	”

Fig. 3 Pore pressure measurements on triaxial samples
Pressions interstitielles dans les échantillons triaxiaux

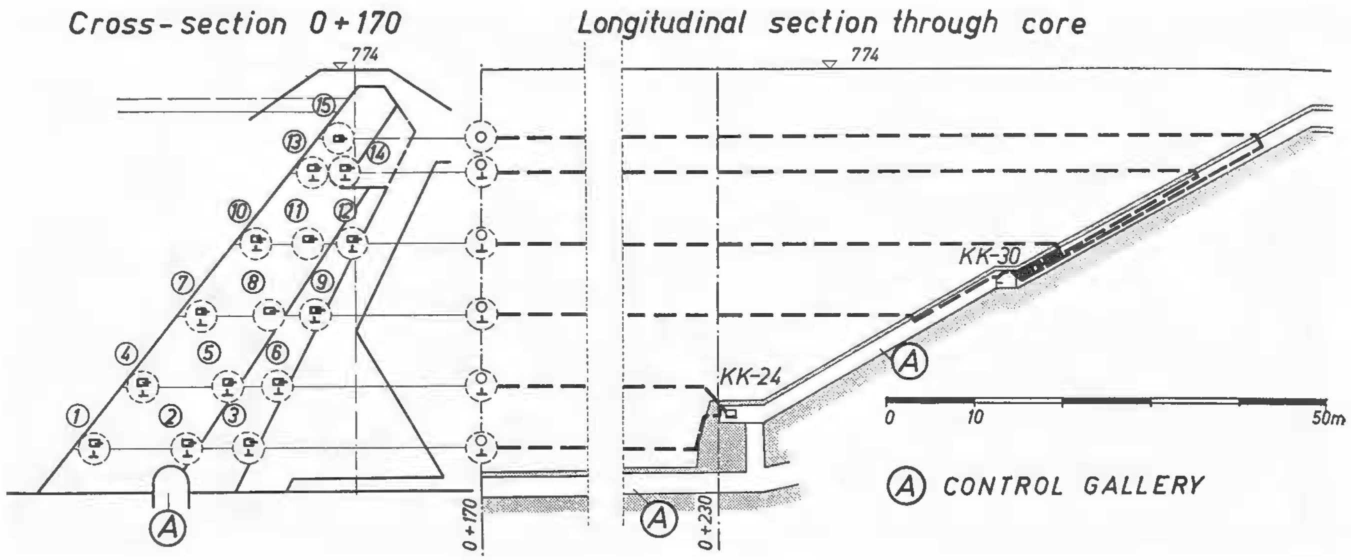

Fig. 4 Locations of piezometers in the core
Emplacement des piésométres dans le noyau

surroundings as well as for the measurement of the stresses and the pore water pressure in the core. Only the installations for the measurement of the pore water pressure will be described, since only this question is being discussed here.

The piezometer cells are placed in two profiles, 20 m apart, in the highest portion of the dam. The arrangement of the cells in the core is shown in Fig. 4. On profile 0 + 170 electro-acoustic piezometers, connected by insulated cables with the measuring stations in the control gallery *A*, have been placed. Here, by means of a switchboard, each cell can be connected with the electro-acoustic measuring device where the pressure can be determined with $\pm$ 0·1 kg/cm^2 accuracy.

Fig. 5 Details of piezometer and earth pressure cells in the core
Point de mesure des pressions interstitielles et des pressions de terre

Altogether 30 manometercells have been placed, two on each point, of which 27 are operating, while 3 have failed although the cable connections remained undamaged. Fig. 5 shows the instruments placed at a measuring point. At profile 0 + 190 piezometer cells have been placed but because of technical difficulties the entire installation has not yet been completed.

Prior to the placement the electro-acoustic manometers were checked in a large oedometer and they produced satisfactory results.

Pore Pressure in the Core

After the installations were placed at the different horizons, readings of the manometers at certain time intervals during the construction and after the filling of the reservoir have been recorded. The excess pressure during construction was small, in accordance with the slow rate of construction and a narrow core. The results of the pore water pressure measurements during construction are not elaborated in detail because simultaneously with the construction of the dam the storage basin was partially filled, so that the recording of the consolidation process during a longer period was not possible.

During the filling of the storage basin the pore water pressure adjusts itself quickly to the water level changes. In Fig. 6 the flow nets of the pore water in the core for three different water levels are given. For comparison the theoretical flow nets drawn for the water level of 26 February 1955 and 28 August 1955 are given in Fig. 7. The difference between the theoretical and measured patterns of the flow nets before and after draw-down is not significant. It is, in the first place, reflected in the deformation of the equipotential lines above the saturation line (phreatic line), because of the pore pressure resulting from the load of the new portion of the dam. This can be seen from the change of the pore pressure after 1 June 1955 when the dam had been raised for more than 6 m on the average. This corresponds to $\Delta\sigma = 11$ t/m^2. The excess pore water pressure in the middle of the core at point 8 amounts to $\Delta u = 5{\cdot}7$ t/m^2, and at point 11 to $\Delta u = 3{\cdot}4$ t/m^2 corresponding to 50 per cent and 30 per cent of the new load respectively.

Between 2 February and 28 August 1955 successive pore pressure measurements in shorter time intervals were performed from which the coefficient $\bar{B}$ can be determined (Skempton 1954; Bishop, 1954).

It is seen from Table 3 that the values of $\bar{B}$ measured in the dam and those from the theoretical flow net for the higher and lower water level agree very well (only point No. 2 does not agree, most probably because of the draining effect of the gallery). The above values refer to relatively small oscillations of the water level in the lake which has not yet been full.

To correlate the results recorded in the dam and in the laboratory the stresses at point No. 4 are also given with the assumption made by Bishop (1954):

$$\gamma_c = 2{\cdot}0 \text{ t/m}^3 \quad \gamma_r = 2{\cdot}1 \text{ t/m}^3 \quad \gamma_{rd} = 1{\cdot}75 \text{ t/m}^3$$

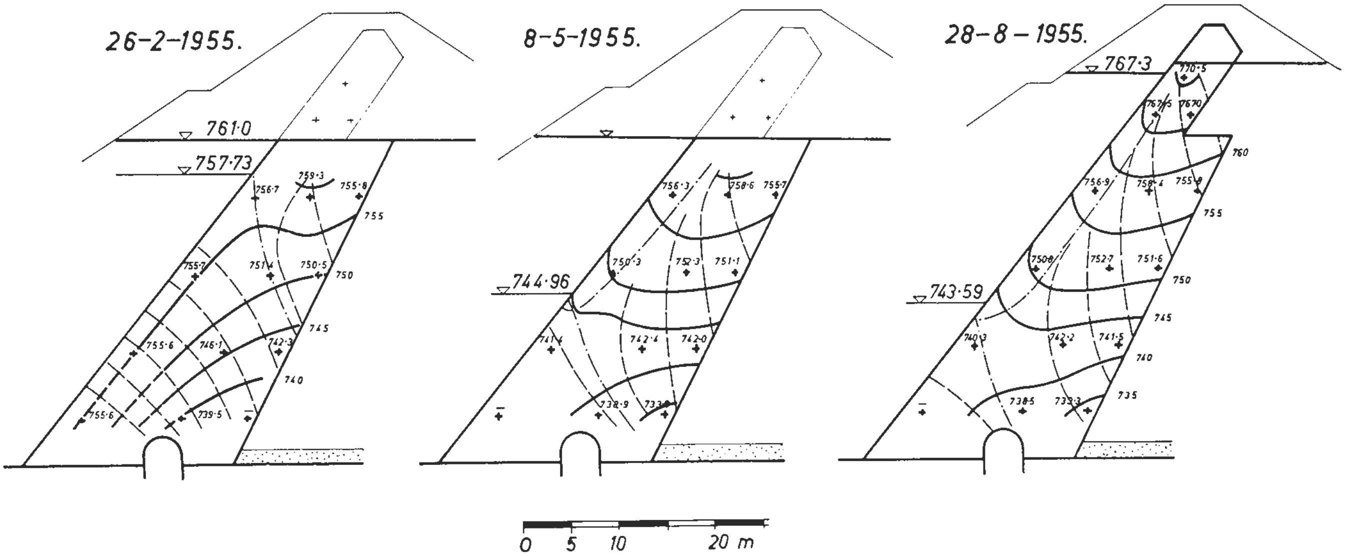

Fig. 6 Measured flow nets—Lokvarka dam
Résaux potentiels mesurés — barrage de Lokvarka

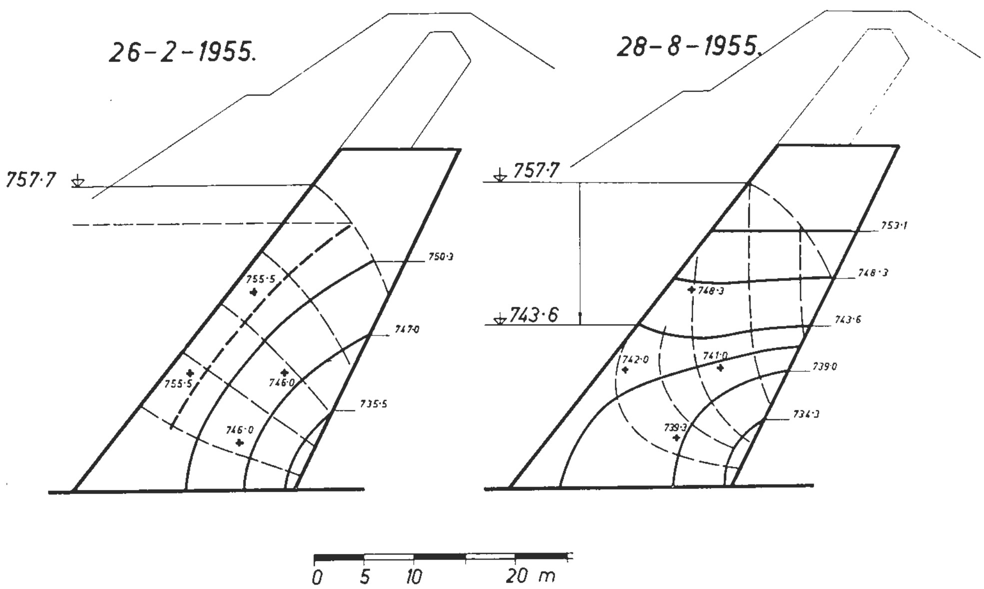

Fig. 7 Theoretical flow nets—Lokvarka dam
Résaux potentiels théoriques — barrage Lokvarka

Table 3
The difference of water levels in the rock dam Δh_w
Différence des niveaux à l'eau dans le remblai rocheux Δh_w

	m	t/m²	*Measurements in dam*				*Theoretical flow net*			
Point	Δh_w	$-\Delta\sigma_1$	u_0	u	$-\Delta u$	$\bar{B}$	u_0	u	$-\Delta u$	$\bar{B}$
2	10·6	3·7	739·5	738·9	0·6	0·16	746·0	739·3	6·7	1·8
4	12·7	4·4	755·6	741·4	14·2	3·2	755·0	742·0	13·5	3·1
5	3·8	1·3	746·1	742·4	3·7	2·8	746·0	741·0	5·0	3·8
7	7·5	2·6	755·7	750·3	5·4	2·1	755·5	748·3	6·7	2·6

$\Delta\sigma_1 = n.\Delta h_w.\gamma_w$

Porosity of the rock-fill $n = 0{\cdot}35$

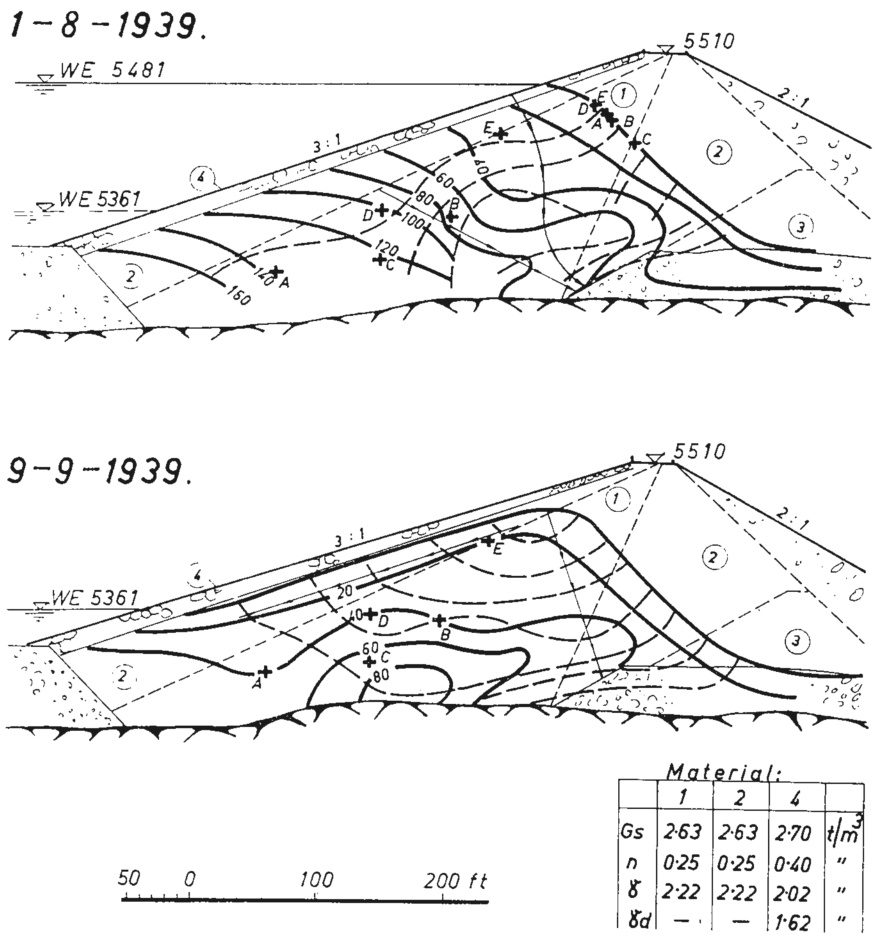

Fig. 8 Measured flow nets—Alcova dam
Pressions d'eau et lignes equipotentielles — barrage d'Alcova

Table 4

Point	h_c	h_r	h_w	h'	$(\sigma_1)_0$	$-\Delta\sigma_1$	u_0	u	$-\Delta u$	$\bar{B}$
A	21·3	3·3	21·3	7·0	75·3	22·5	38·9	12·2	26·7	1·19
B	22·0	2·7	7·0	14·0	61·4	8·1	17·0	12·2	4·8	0·59
C	26·0	3·0	13·0	8·5	76·7	14·2	33·5	20·7	12·8	0·90
D	14·0	3·0	13·0	4·6	51·5	14·4	26·0	12·2	13·8	0·96
E	6·3	2·4	3·3	4·6	22·1	4·2	7·4	3·6	3·8	0·90
K	15·5	1·8	6·8	3·0	40·4	6·7	20·0	12·2	7·8	1·16

(all dimensions in m and t)

Water level 757·33:

$$h_c = 2{\cdot}8 \quad h_r = 15{\cdot}7 \text{ m} \quad h_{rd} = 3{\cdot}8 \text{ m}$$

$$(\sigma_1)_0 = 45{\cdot}2 \text{ t/m}^2 \text{ (64·5 lb./sq. in.)}$$

$$u_0 = 18{\cdot}5 \text{ t/m}^2 \text{ (26·4 lb./sq. in.)}$$

Water level 744·96:

$$h_c = 2{\cdot}8 \quad h_r = 3{\cdot}0 \text{ m} \quad h_{rd} = 16{\cdot}5$$

$$\sigma_1 = 40{\cdot}8 \text{ t/m}^2 \text{ (58 lb./sq. in.)}$$

$$\Delta\sigma_1 = -4{\cdot}4 \text{ t/m}^2 \text{ (6·5 lb./sq. in.)}$$

The vertical stress is approximately equal to that of the laboratory sample, while the reduction $\Delta\sigma_1$ is smaller than in the laboratory sample. The corresponding pore pressure coefficient from the laboratory tests would be, according to Fig. 3, *c* for $(\sigma_1 + \Delta\sigma_1):\sigma_1 = 40{\cdot}8:45{\cdot}2 = 0{\cdot}91$, $\bar{B} = 2{\cdot}1$. This is lower than measured in the dam; the pore pressure change in the core computed from this $\bar{B}$ value would be smaller and the excess pore pressure higher.

A good agreement between the actual and the theoretical pattern of the flow nets for the rapid draw-down case can be detected from the data published for some other dams. As an example the equal pressure and equipotential lines in the Alcova Dam (U.S. Bureau of Reclamation, 1951) for a rapid draw-down are given in Fig. 8. The characteristics of the materials were taken from Daehn and Hilf (1951) publication. For the points marked with *A–E* the $\bar{B}$ values were calculated as shown in Table 4; *K*, refers to the flow net in Fig. 9.

In Fig. 9 the theoretical flow nets for a full and empty storage

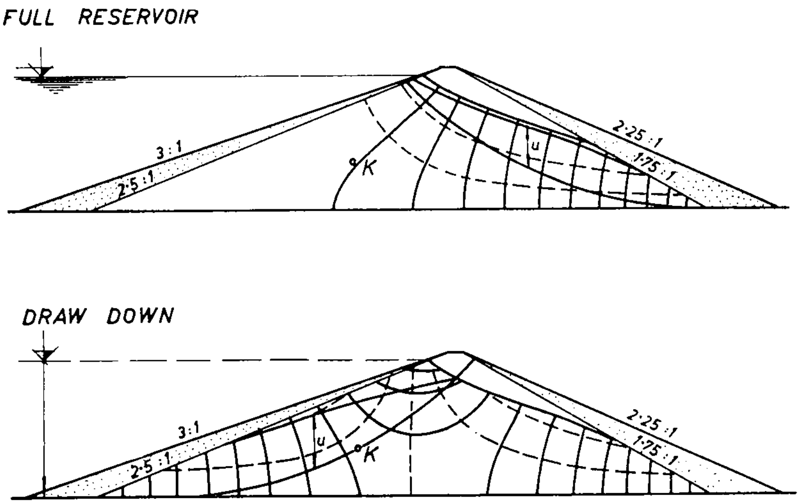

Fig. 9 Theoretical flow nets—dam with wide core
Résaux potentiels théoriques — barrage avec noyau large

basin of a similar dam with a wide core are given. The value of $\bar{B}$ for the point K is also given in Table 4. This example also shows that the coefficients $\bar{B}$ computed from the measured and the theoretical flow nets are of the same order of value.

From the data, as well as from flow nets recorded on some other dams, the conclusion could be drawn that at rapid draw-downs the flow net quickly adjusts itself to the new border conditions according to the laws for flow of ground water in the gravitational field. This result is opposite to the wide-spread opinion that the magnitude of the pore pressure after rapid draw-down depends primarily on the characteristic of the material (Bjerrum, 1953; Mayer and Habib, 1955) but is well in agreement with the tests by Breth (1954), and the theoretical considerations of Glover, Gibbs and Daehn (1948).

It seems that it is easier and more dependable to compute the pore pressures after a rapid draw-down from the corresponding flow nets than from laboratory measurements of the coefficient $\bar{B}$. For dams where the core is built of well compacted clay of low compressibility this procedure gives pore pressures in accordance with those measured in actual dams.

Further publication of measurements in actual dams, especially with cores of more compressible clay, would be of great value for the definite clarification of the pore pressure changes occurring after rapid draw-downs.

References

Bishop, A. W. (1954). The use of pore pressure coefficients in practice. *Géotechnique*, **4**, No. 4, 148

Bjerrum, L. (1953). Stability and deformation of slopes, earth dams and groundwater problems. *General Report Proc. 3rd International Conference on Soil Mechanics and Foundation Engineering*, Vol. 2, Zürich

Breth and Kückelmann (1954). Der Porenwasserdruck in Erddammen, *Bautechnik*. Berlin, No. 1

Daehn, W. W. and Hilf, J. W. (1951). Implications of pore pressure in design and construction of rolled earth dams. *Trans. 4th Congress on Large Dams*, R.39, New Delhi

Glover, R. E., Gibbs, H. J. and Daehn, W. W. (1948). Deformability of earth materials and its effect on the stability of earth dams following a rapid drawdown. *Proc. 2nd International Conference on Soil Mechanics and Foundation Engineering*, Rotterdam, Vol. 5, p. 77

Mayer, A. and Habib, P. (1955). Note sur les variations des sous-pressions dans les massifs à faible perméabilité. *Géotechnique*, **5**, No. 2

Nonveiller, E. (1954). *Prikaz projekta i gradjenja nasute pregrade Lokvarka, Saopšt. II. savj. vis. brane Jugoslavonske sekcije medjunar. komisije za Visoke brane.* Beograd

Skempton, A. W. (1954). The pore pressure coefficients A and B. *Géotechnique*, **4**, No. 4

U.S. Bureau of Reclamation (1950). Treatise on dams, design supplement No. 2, vol. X. *Design and Construction Reclamation Manual*, Fig. 6